EXPERIMENTAL ANALYSIS OF RJL-1, CHINESE FORCE BALANCE ACCELEROMETER

by

Ali Amini[1], Owen Hata[2] and Mihailo Trifunac[2]

ABSTRACT

Theoretical and experimental analyses of Chinese Force Balance Accelerometer (RJL-1), manufactured by the Institute of Engineering Mechanics, SSB in Harbin, are presented. It is found that the transfer function of this transducer is identical to the American Force Balance Accelerometer (FBA-1). It is also observed that the representation of the transducer response by means of a single degree of freedom viscously damped system for frequencies near and higher than its natural frequency, is not adequate.

1. Introduction

Force-balance transducers (FBT) possess an electrical feedback loop which maintains the transducer mass in the state of equilibrium. An input force (caused by the absolute base acceleration) is balanced by an opposing force exerted on the mass by a force generator. An electrical pick-up (usually of capacitive type) is used to sense the relative motion of the mass and its output is fed to the force generator. This allows the FBT to achieve a wider frequency response range than a conventional open-loop transducer.

Damping can be achieved through either a phase-shifting network or a velocity sensing pick-up in the feedback loop. Both damping and natural frequency can be adjusted and altered by changing the electrical components in the circuit of the feedback loop. The mechanical stiffness and the damping are typically negligible compared with the electrically produced

1 School of Engineering, CSUN, Dept. of Electrical and Computer Engineering, 18111 Nordhoff St., Northridge, CA 91330 USA.

2 School of Engineering, USC, Dept. of Civil Engineering, University Park, Los Angeles, CA 90098—2531 USA.

equivalent terms and are often ignored in the equilibrium analysis of the transducer vibrating mass.

The operating principle of an FBT may be better understood by considering a typical block diagram (Figure 1) and its input-output relations.

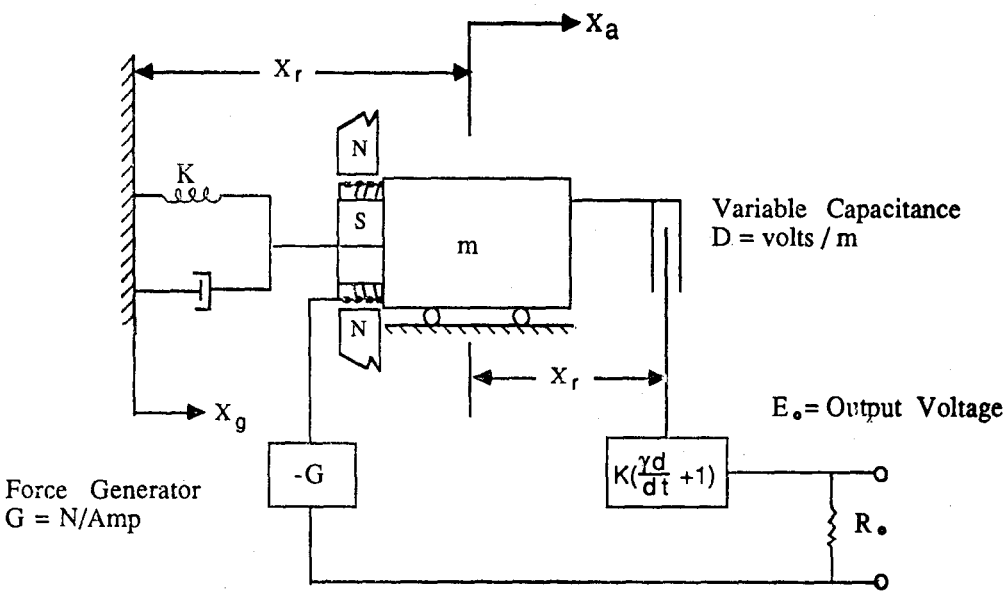

Figure 1 Force Balance Accelerometer Block Diagram

Ground acceleration, applied along the axis of the FBT, causes the mass to move relative to a fixed reference. The pick-up device (variable capacitance with sensitivity of D(V/m)) senses this motion producing a voltage output which is fed to an amplifier of gain K and a velocity sensing pick-up, or a phases-advancing network with transfer function $(1+\gamma d/dt)$. The output current i(amp) is then fed to a force generator G(N/amp) which generates the necessary force needed to balance the inertia force produced by the acceleration.

Hudson[2] studied the system shown in Figure 1 and derived the following equations:

$$\ddot{X}_a = \ddot{X}_r + \ddot{X}_g \tag{1}$$

with

$$m\ddot{X}_r + \left(C + \frac{DKG\gamma}{R_0}\right)\dot{X}_r + \left(K + \frac{DKG}{R_0}\right)X_r = -m\ddot{X}_g \tag{2}$$

or

$$\ddot{X}_r + 2\omega_n\zeta\dot{X}_r + \omega_n^2 X_r = -\ddot{X}_g \tag{3}$$

where

$$2\omega_n\xi=\left(\frac{C}{m}+\frac{DKG\gamma}{mR_0}\right), \tag{4}$$

$$\omega_n^2=\left(\frac{K}{m}+\frac{DKG}{mR_0}\right), \tag{5}$$

and the output voltage is

$$E_0=DK(X_{\tilde{t}}+\gamma\dot{X}_{\tilde{t}}). \tag{6}$$

Assuming sinusoidal ground acceleration

$$\ddot{X}_{\tilde{g}}=a_g\sin\omega t \tag{7}$$

and taking into account the fact that the mechanical stiffness K and the damping constant C are small compared to the electrical stiffness DKG/R_0 and damping $DKG\gamma/R_0$, the instrument response becomes:

$$E_0=\left(\frac{mR_0}{G}\right)a_{\tilde{g}}A\sin(\omega t-\phi), \tag{8}$$

where

$$A=\frac{\sqrt{1+\left[2\left(\frac{\omega}{\omega_n}\right)\xi\right]^2}}{\sqrt{\left[1-\left(\frac{\omega}{\omega_n}\right)^2\right]^2+\left[2\left(\frac{\omega}{\omega_n}\right)\xi\right]^2}} \tag{9}$$

and the phase shift ϕ is

$$-\phi=\arctan\frac{2\left(\frac{\omega}{\omega_n}\right)^3}{1+\left(\frac{\omega}{\omega_n}\right)^2(4\xi^2-1)} \tag{10}$$

Hudson's work shows that the advantages of the force-balance transducers are: (1) the broadening of the frequency response range; and (2) the ability to alter the natural frequency or damping of the transducer by changing the electrical components in the feedback loop.

2. Theoretical Analysis

The circuit diagram of the Force Balance Accelerometer RJL-1 is shown in Figure 2. It is observed that with the exception of the numbering system, the circuit of the Chinese RJL-1 is identical to the Kinemetrics FBA-1 (Amini and Trifunac, 1985). The electrical pick up is a variable capacitor. Modulation and demodulation are used to sense and recover the data. The velocity sensing pick-up, used for damping, is a combination of the electrical components and voltage induced in the coil in the feedback loop of the circuit. The current that flows through L is the current that balances the

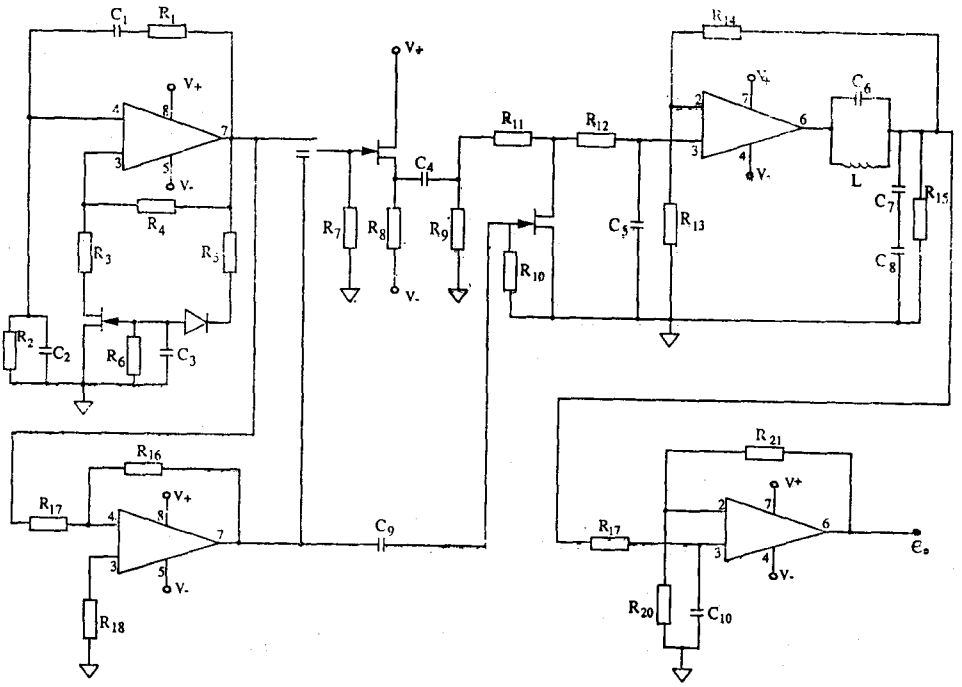

Figure 2 Circuit Diagram of Force Balance Accelerometer RLJ-1(Courtesy of IEM)

force. Amplification is performed at two stages and two low pass filters are present in the circuit. From the results of Amini and Trifunac[1], the output voltage of RJL-1 in S domain can be written as:

$$E_0(s)=\frac{R_{20}+R_{21}}{R_{20}}\cdot\frac{R_{14}+R_{13}}{R_{13}}\cdot\frac{1}{1+R_{17}C_{10}s}\cdot \cdot\frac{1}{1+R_{12}C_5 s}\cdot\frac{-DA(s)\cdot A^*}{s^2+2\zeta\omega_n s+\omega_n^2} \tag{11}$$

and the transfer function as:

$$H(s)=\frac{E_0(s)}{A(s)} \tag{12}$$

The term $A(s)$ is the acceleration in S domain,

$$A^*\simeq 1 \tag{13}$$

$$2\zeta\omega_n\simeq\frac{DGC^*}{M}\,\frac{R_{14}+R_{13}}{R_{13}} \tag{14}$$

$$\omega_n^2\simeq\frac{DG}{M}\,\frac{R_{15}+R_{14}+R_{13}}{R_{13}R_{15}} \tag{15}$$

and

$$C^*=\frac{C_7C_8}{C_7+C_8} \tag{16}$$

In the above equation M is the mass, G in N/amp is the generator force

constant and D, in V/m, is the variable capacitor sensitivity.

In equation (11) both low-pass filters and amplifications are included, and so the system is represented by a fourth order rather than by a second order equation. This is particularly important for frequencies around and greater than the natural frequency of the transducer.

Comparing this result with that of Hudson[3], basic differences in amplification and in phase become apparent. In the analysis of RJL-1 the output voltage is proportional to the relative displacement only, and the 90° phase shift produces electrical damping, while the velocity $\dot{x}$, is itself not part of the output. The system acts as a single-degree-of-freedom system for low frequencies. In Hudson's model the output voltage is proportional to both the relative displacement x, and the velocity $\dot{x}$. The RJL-1 acts like a conventional transducer, but with a higher corner frequency due to the feedback loop.

For low frequencies (<40 Hz) the transducer output voltage $E_0(s)$ can be written as

$$E_0(s) = \frac{R_{20}+R_{21}}{R_{20}} \cdot \frac{R_{14}+R_{13}}{R_{13}} \cdot \frac{-DA(s)}{s^2+2\zeta\omega_n s+\omega_n^2} \tag{17}$$

with the transfer function defined by

$$H(s) = \frac{E_0(s)}{A(s)}. \tag{18}$$

3. Experimental Analysis

Shaking table tests were performed, producing the system transfer function, and RJL-1 was compared with another transducer having corner frequency higher than the maximum testing frequency. Both transducers were mounted on the shaking table and subjected to random and sinusoidal excitation.

Procedure

An Endevco accelerometer (2262M9-YQ02) was used as the reference accelerometer. It has a mounted resonance frequency of 2500Hz and a flat frequency response in the range of 0 to 750 Hz.

The equipment used for this test consisted of the following:

1. a+/−12VDC power supply to power the RJL-1 (the voltage and current used to power the RJL-1 were measured to be +12.7 and −12.8VDC, and 13mA);

2. Tektronix 502A oscilloscope to monitor data from the transducers;

3. Hewlett-Packard 3582A Spectrum Analyzer to analyze test data;

4. Hewlett-Packard 7015B X-Y plotter to plot the transfer and coherence functions of RJL-1 with respect to the reference accelerometer, the frequency spectrum of both transducers and the time history of RJL-1;

5. Electro-SEIS shaker (model 113) manufactured by Acoustic Power Systems Inc;

6. Wavetek VCG114 function generator to generate sinusoidal wave signals; and

7. Unkelscope by Unkel Software Inc. to analyze the sinusoidal test data.

Two forms of excitation were utilized in this experiment (random and sinusoidal). The HP3582A Spectrum Analyzer was used to produce the random excitation signal, which contains all frequencies in the range of interest (0 to 100Hz). The Wavetek function generator was used to generate sinusoidal waves at discrete frequencies, from 4 to 100Hz, in increments of 4 Hz. The spectrum analyzer was used to check the frequency of the sinusoidal excitation.

A block diagram of the experimental set-up is shown in Figure 3.

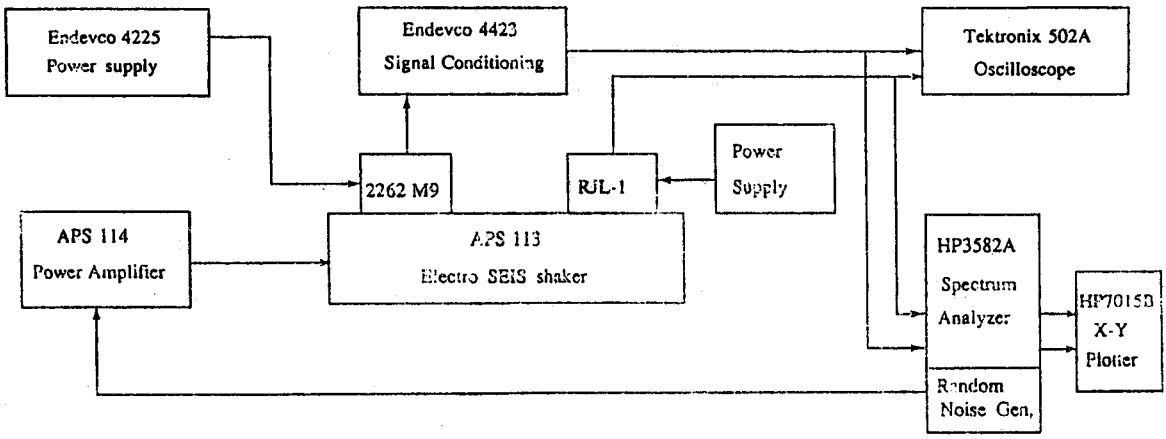

Figure 3 Shaking Table Test Block Diagram.

For random excitation the transfer function of the RJL-1 with respect to the Endevco accelerometer was obtained from an HP3582A Spectrum Analyzer. The coherence function between the RJL-1 and the Endevco accelerometer was also computed by the spectrum analyzer.

Since the Endevco accelerometer has a flat frequency response from 0 to 750 Hz and the test frequency range is 0 to 100 Hz it is reasonable to assume that the ratio of the Fourier Transform of the RJL-1 output to that of the Endevco accelerometer results in the transfer function of the RJL-1.

The results of the test were recorded on an HP3582A and plotted

using an HP7015B X-Y plotter. The transfer function was obtained at discrete frequencies by dividing the peak to peak output of the RJL-1 by the peak to peak output of the Endevco accelerometer.

A static calibration of the instrument was carried out by rotating it through 90° and recording its output. The sensitivity of the RJL-1 was determined in this way to be approximately 5V/g. This was verified when a 2g input (8Hz sine wave) produced a full scale (+/−10V) output.

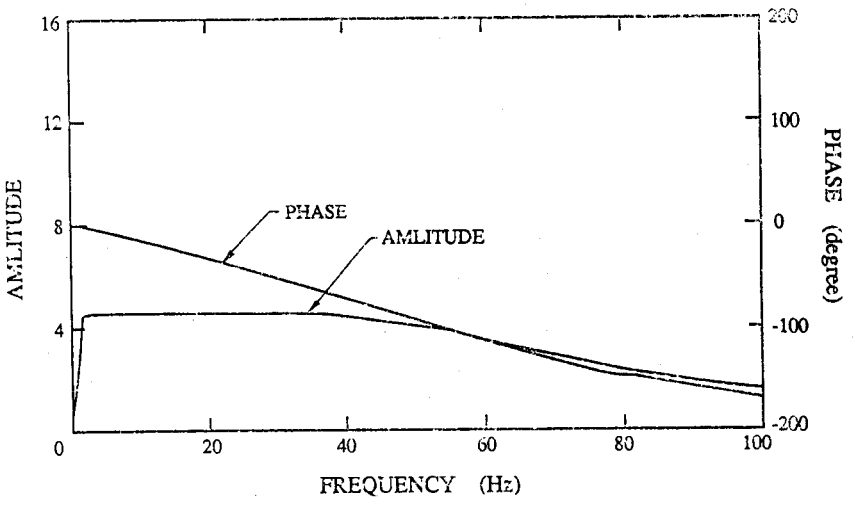

Figure 4 Transfer Function of RJL-1 with Respect to Endevco(2262Mq). Excitation is Random Noise.

Results

Figure 4 shows the transfer function of the RJL-1 obtained from a random noise excitation with respect to the Endevco accelerometer. The coherence function between the outputs of the two accelerometers was computed using the spectrum analyzer. The coherence function indicates good accuracy of the results in the range from 4 to 100 Hz. Table 2 gives the amplitudes and phase of the transfer function at discrete frequencies, taken from HP3582A. Table 3 lists the amplitudes of the transfer function at discrete frequencies, obtained through sinusoidal wave excitations, along with the results of random noise excitation tests. Figure5 compares the transfer functions obtained with random noise and with sinusoidal wave excitation. As it can be seen, there is a good agreement between the two different excitations.

The test results indicate that the transfer function of the RJL-1 is flat in the range 0 to 30 Hz before the roll-off occurs. The natural frequency and damping of the RJL-1 were determined by evaluting the square of the

Table 1 RJL-1 Accelerometer Calibration Data (Courtesy of IEM.)

Measurement Range	±1.5g
Sensitivity	5v/g
Dynamic Range	100db
Noise Level	≤50/v
Damping Constant	0.65
Natural Frequency	60Hz.
Frequency Range	0—65Hz(3db)
Transversal Sensitivity	1 %g/g
Humidity	85%
Size	6 × 7 × 8cm³
Permitted Temperature	-10℃—50℃
Weight	750g

Table 2 Experimental gain and phase shift (random test)

freq(Hz)	amplitude	phase(deg)
4.0	4.78	- 8
8.0	4.77	- 15
12.0	4.77	- 22
16.0	4.77	- 30
20.0	4.77	- 36
24.0	4.74	- 44
28.0	4.78	- 51
32.0	4.75	- 60
36.0	4.67	- 68
40.0	4.57	- 77
44.0	4.44	- 86
45.3	4.37	- 89
46.4	4.34	- 92
48.0	4.25	- 95
52.0	4.03	- 1.4
56.0	3.79	- 113
60.0	3.53	- 121
62.4	3.37	- 126
64.0	3.26	- 129
68.0	3.01	- 136
72.0	2.78	- 143
76.0	2.47	- 151
80.0	2.22	- 155
84.0	2.04	- 160
88.0	1.86	- 165
92.0	1.70	- 169
96.0	1.58	- 174
100.0	1.46	- 178

error between the experimentally determined transfer function and a single-degree-of-freedom system transfer function (equation 17) for different natural frequencies and fractions of critical damping. The minimum error

Table 3 Experimental gain (random and sine wave excitations)

freq(Hz)	Amplitude	
	random	sine
4.00	4.78	4.69
8.00	4.77	4.70
12.00	4.77	4.74
16.00	4.77	4.77
20.00	4.77	4.72
24.00	4.74	4.72
28.00	4.78	4.75
32.00	4.75	4.73
36.00	4.67	4.63
40.00	4.57	4.55
44.00	4.44	4.39
48.00	4.25	4.23
52.00	4.03	3.97
56.00	3.79	3.77
60.00	3.53	3.53
64.00	3.26	3.24
68.00	3.01	2.98
72.00	2.78	2.77
76.00	2.47	2.48
80.00	2.22	2.24
84.00	2.04	2.07
88.00	1.86	1.87
92.00	1.70	1.73
96.00	1.58	1.59
100.00	1.46	1.46

obtained was for values $f_n = 56.0$Hz and $\xi = 0.64$. The transfer function of a single-degree-of-freedom system with the above values for f_n and ξ is plotted along with the transfer function of the RJL-1 obtained experimentally (Figure6).

The square of the difference between the shaking test transfer function result and equation 11 (disregarding amplification factors) was also obtained for different natural frequencies and damping values. The values obtained for this case were $f_n = 61$Hz and $\xi = 0.63$. The transfer function amplitudes of equation 12 with these optimum values are shown in Figure 6. Figure 7 shows phase shift versus frequency for the theoretical and the experimental responses. Note that the natural frequency and the damping value indicated in the calibration data of Table 1 are 60 Hz and 0.65 respectively.

The magnitude of the single-degree-of-freedom system transfer function agrees with the experimental results, while the phase shift differs appreciably. This is due to the shift in phase introduced by the low-pass filters.

The transfer function obtained from equation (11) is in very close agreement with the shaking test results.

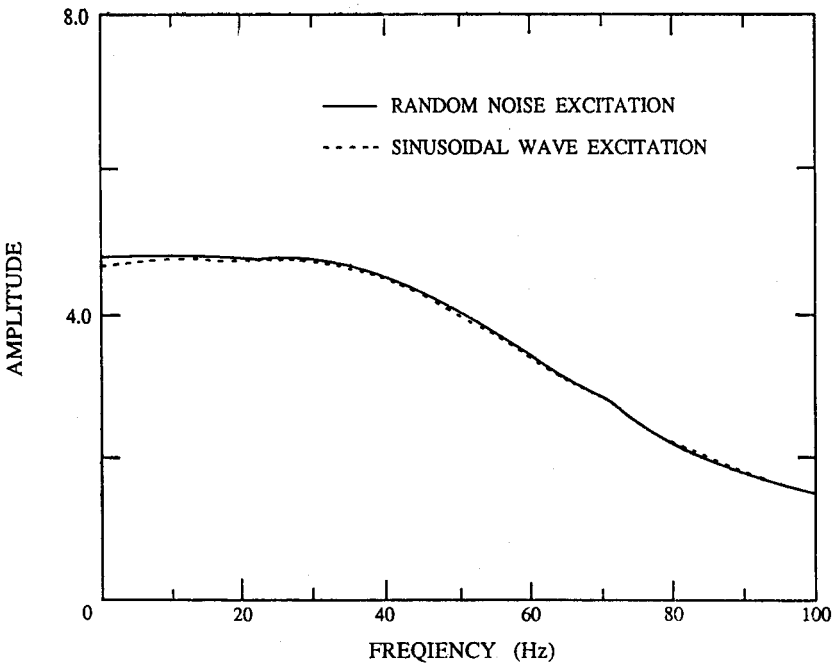

Figure 5 Transfer Function Amplitude of RJL-1

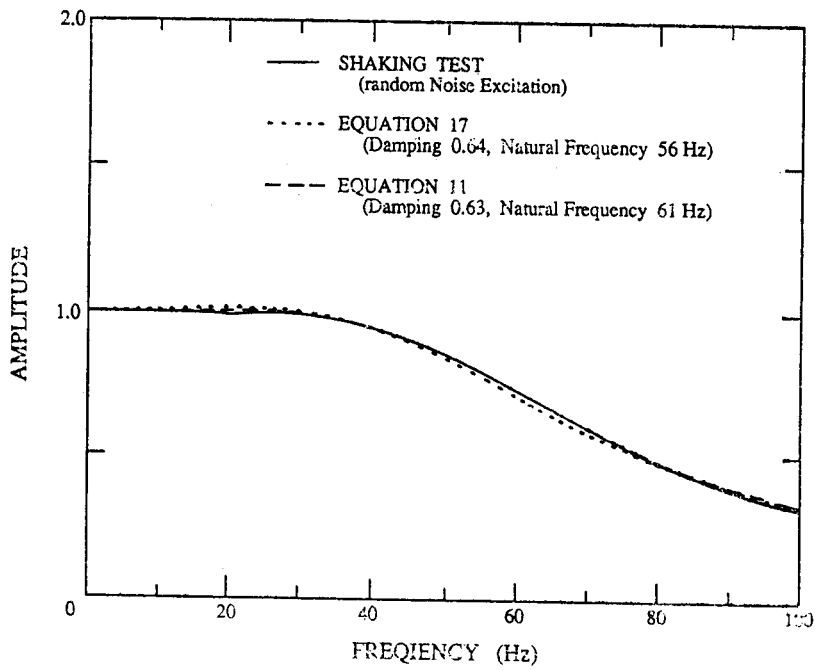

Figure 6 Transfer Function Amplitude (Normalized) of RJL-1

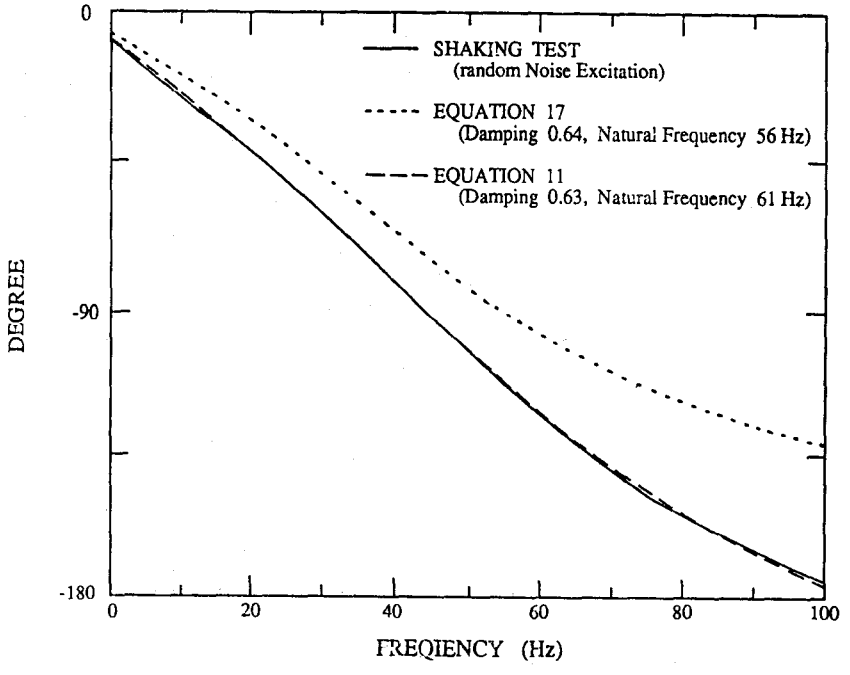

Figure 7 Phase Shift of RJL-1 Versus Frequency

4. Conclusions

Based on the above theoretical and experimental analyses, the following conclusions can be stated:

1. The output of RJL-1 (voltage E_0) is directly proportional to the relative displacement X_r only. This produces a response similar to that of conventional transducers.
2. The circuit and the transfer function characteristics of IEM RJL-1 are practically identical to those of Kinemetrics FBA-1. The only difference is that the RJL-1 has a higher corner frequency, smaller size and less weight than the FBA-1.
3. The shaking test results indicate that the RJL-1 should be represented by a fourth order system just as the FBA-1[1]. The best fit curve to the shaking test result is obtained from equation (11) with damping of 0.65 and natural frequency of 60 Hz. The second order system model of the RJL-1 (equation (17)) may be used only for frequencies below 40 Hz. This is also apparent in Figures 6 and 7.
4. It is seen from equation (15) that the square of the natural frequency is inversely proportional to R_{15} and directly proportional to R_{14}. The value of R_{13} is normally kept constant. Equation (14) indicates that the

product of natural frequency and damping is directly proportional to R_{14}. The main part of the critical damping is produced by the capacitor C^* (equation 16).

References

[1] Amini,A.,and Trifunac M.D., Analysis of a Force Balance Accelerometer, Soil Dynamics and Earthquake Engineering, 1985, Vol.4, No.2,82—90.

[2] Hudson, D.E., Unpublished notes and personal communication,(1979).

[3] Neubert,Herman K., Instrument Transducers: An Introduction to Their Performance and Design, Oxford,Clarendon,Press,1975(2nd ed.).

[4] Norton,Harry N.,Handbook of Transducers for Electronic Measuring Systems, Englewood Cliffs,N.J., Prentice Hall,1969.

[5] Oliver, Frank J.,Practical Instrumentation Transducers, New York, Hayden Book Co.,1971.

中国 RJL-1力平衡加速度计的实验分析

Ali Amini

(美国诺恩里奇加州州立大学电机与计算机工程系)

Owen Hata

(美国南加州大学土木工程系)

Mihailo Trifunac

(美国南加州大学土木工程系)

提 要

本文给出哈尔滨国家地震局工程力学研究所制造的中国力平衡加速度计 (RJL-1) 的理论和实验分析。研究发现，此传感器的传递函数与美国的力平衡加速度计 (FBA-1)相同。同时观察到，用单自由度粘滞阻尼体系表示传感器的反应，对于接近于和高于自振频率的频率是不适当的。